The Astrophysical Journal Letters, 917:L39 (5pp), 2021 August 20 https://doi.org/10.3847/2041-8213/ac1b2f

Cosmic-Ray Acceleration from Turbulence in Molecular Clouds

Brandt A. L. Gaches[1,2], Stefanie Walch[1,3], and A. Lazarian[4]
[1] I. Physikalisches Institut, Universität zu Köln, Zülpicher Straße 77, D-50937, Köln, Germany; gaches@ph1.uni-koeln.de
[2] Center of Planetary Systems Habitability, The University of Texas at Austin, TX, USA
[3] Center for Data and Simulation Science, Universität zu Köln, Köln, Germany
[4] Department of Astronomy, University of Wisconsin-Madison, WI, USA
Received 2021 June 25; revised 2021 August 5; accepted 2021 August 5; published 2021 August 24

Abstract

Low-energy cosmic rays, in particular protons with energies below 1 GeV, are significant drivers of the thermochemistry of molecular clouds. However, these cosmic rays are also greatly impacted by energy losses and magnetic field transport effects in molecular gas. Explaining cosmic-ray ionization rates of $10^{-16}\,s^{-1}$ or greater in dense gas requires either a high external cosmic-ray flux, or local sources of MeV–GeV cosmic-ray protons. We present a new local source of low-energy cosmic rays in molecular clouds: first-order Fermi acceleration of protons in regions undergoing turbulent reconnection in molecular clouds. We show from energetic-based arguments there is sufficient energy within the magnetohydrodynamic turbulent cascade to produce ionization rates compatible with inferred ionization rates in molecular clouds. As turbulent reconnection is a volume-filling process, the proposed mechanism can produce a near-homogeneous distribution of low-energy cosmic rays within molecular clouds.

Unified Astronomy Thesaurus concepts: Molecular clouds (1072); Cosmic ray sources (328); Cosmic rays (329); Astrochemistry (75)

1. Introduction

Molecular clouds are immersed in a bath of cosmic rays (CRs), i.e., energetic charged particles that are accelerating and propagating in our Galaxy (Schlickeiser 2002). Low-energy particles, particularly protons with energies between 1 MeV and 1 GeV, influence the thermochemistry of molecular gas in regions which are well shielded from ultraviolet radiation (see reviews by Dalgarno 2006; Padovani et al. 2020). The chemistry of cold molecular gas is regulated through ion–neutral reactions. Ion–neutral chemistry is largely initiated following the ionization of H_2 and subsequent production of H_3^+:

$$H_2 + H_2^+ \rightarrow H_3^+ + H. \quad (1)$$

Deuterium chemistry is also regulated in a similar manner through the production of H_2D^+ from HD. The CR ionization rate (CRIR), ζ, is inferred primarily through molecular line features from ions, such as H_3^+, OH^+, and H_nO^+ absorption and emission from species such as HCO^+, DCO^+, and N_2H^+. These observations have shown that the CRIR in diffuse molecular gas spans $10^{-16} < \zeta < 10^{-15}\,s^{-1}$ (e.g., Indriolo & McCall 2012; Indriolo et al. 2015; Neufeld & Wolfire 2017). In the dense gas, observations infer the CRIR in a wider range from $10^{-17} < \zeta < 10^{-15}\,s^{-1}$ (e.g., Caselli et al. 1998; Favre et al. 2017; Barger & Garrod 2020). Recently, observations and astrochemical models have inferred a CRIR toward the protocluster OMC-2 FIR 4 of approximately $\zeta \approx 10^{-14}\,s^{-1}$ (Ceccarelli et al. 2014; Favre et al. 2018).

One-dimensional models of transport through molecular gas conflict with the heightened ionization rates inferred in shielded, dense gas. These models ubiquitously predict a declining CRIR with column density, $\zeta(N)$, whether due to energy losses[5] or magnetic field effects[6] (Padovani et al. 2009; Morlino & Gabici 2015; Schlickeiser et al. 2016; Ivlev et al. 2018; Phan et al. 2018; Silsbee & Ivlev 2019; Fujita et al. 2021). A dense gas CRIR similar to that inferred in diffuse gas may necessitate a source of low-energy CRs within the gas. Some of these sources have already been posited, such as protostellar jets (Padovani et al. 2016), protostellar accretion shocks (Padovani et al. 2016; Gaches & Offner 2018), H II regions (Meng et al. 2019; Padovani et al. 2019), and embedded stellar winds (Yang & Wang 2020). These are localized sources of CR acceleration that are expected to induce rather inhomogeneous distributions of CRs within molecular clouds.

We propose a new source of low-energy CRs in dense magnetized molecular clouds: particles accelerated within zones of turbulent reconnection. Turbulence is known to be part and parcel of the molecular cloud dynamics (McKee & Ostriker 2007) and it is known to be accompanied by fast turbulent reconnection (Lazarian & Vishniac 1999; Eyink et al. 2011, 2013). The latter process is known to induce the acceleration of energetic particles (de Gouveia dal Pino & Lazarian 2005; Kowal et al. 2011; Lazarian et al. 2020).

We explain in Section 2 our simplified model of CR production in reconnection zones in magnetohydrodynamic (MHD) turbulence. Section 3 presents the results of these calculations and discusses the broad implications of the mechanism.

2. Method

We assume a spherical, magnetized, hierarchical cloud with MHD turbulence. MHD turbulence is injected at some large scale, L, with a velocity dispersion, σ_0, and cascades through the cloud. Figure 1 gives a schematic of the proposed

[5] The dominant energy losses for 1 MeV–1 GeV protons are due to ionizing atomic and molecular material and the production of pions.

[6] Magnetic field effects such as screening, mirroring, and streaming instabilities.

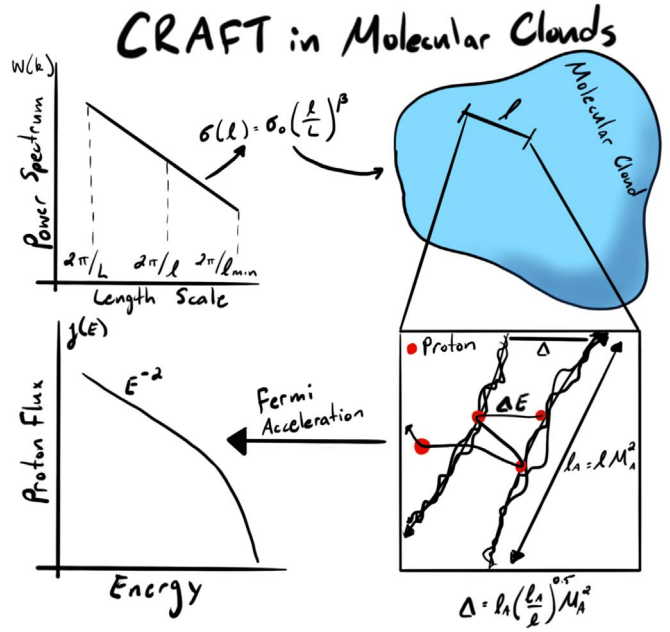

Figure 1. Basic schematic of the proposed mechanism. Top left: we assume a power-law power spectrum related to a line width–size relation. Top right: the turbulence driven at scale, ℓ, corresponds to an average density and magnetic field "seen" by the turbulence. Bottom right: Within the turbulence there are reconnection regions of width Δ (Equation (18)). Here, protons bounce between the reconnection fronts. Bottom left: the resulting acceleration, via the Fermi mechanism, results in a power-law energy distribution.

mechanism. At a given length scale, ℓ, the turbulent line width is given by the line width–size relation (Larson 1981; McKee & Ostriker 2007; Heyer & Dame 2015)

$$\sigma(\ell) \approx \sigma_0 \left(\frac{\ell}{L}\right)^{\beta} \tag{2}$$

where we use $\beta = 0.5$. The density of the gas is calculated by assuming the gas can be prescribed by the virial parameter, α_V, defined by

$$\alpha_V = \frac{5\sigma^2 \ell}{GM} \tag{3}$$

where G is the gravitational constant. The density is thus

$$\rho = \frac{15}{4\pi G \alpha_V}\left(\frac{\sigma^2}{\ell^2}\right). \tag{4}$$

Finally, the magnetic field is calculated using the empirical fit from Crutcher & Kemball (2019)

$$B(n) = \begin{cases} B_0 & n \leqslant n_0 \\ B_0 \times \left(\frac{n}{n_0}\right)^{\kappa} & n > n_0 \end{cases} \tag{5}$$

where $n = \rho/(2.33 \times m_H)$ is the number density, $B_0 = 10\,\mu$G, $n_0 = 300\,\mathrm{cm}^{-3}$, and $\kappa = 0.65$.

The energy within the MHD turbulence cascade depends on the Alfvén Mach number, $\mathcal{M}_{\rm A} = \sigma(\ell)/v_{\rm A}$ where $v_{\rm A}$ is the Alfvén speed, $v_a = \frac{B}{\sqrt{4\pi\rho}}$. In the ideal MHD case, the dissipation rate of the specific energy per unit mass is given by Lazarian et al. (2020)

$$\epsilon = \begin{cases} \frac{\sigma^3}{\ell} & \mathcal{M}_{\rm A} \geqslant 1 \\ \frac{\sigma^4}{v_{\rm A}\ell} & \mathcal{M}_{\rm A} < 1. \end{cases} \tag{6}$$

The dissipation rate of energy per unit volume is then $\varepsilon = \rho\epsilon$. A fraction of this energy, $f_{\rm CR}$, goes into CR acceleration, such that

$$\varepsilon_{\rm CR} = f_{\rm CR}\,\varepsilon, \tag{7}$$

where we take $f_{\rm CR} = 0.01$ as an estimated lower limit of the acceleration efficiency. We assume particles are accelerated within the turbulent reconnection regions via a first-order Fermi process (de Gouveia dal Pino & Lazarian 2005). Following Khiali et al. (2015), the CRs are isotropically injected with an exponentially suppressed power law

$$Q(E) = Q_0 E^{-\gamma} e^{-\frac{E}{E_0}} \tag{8}$$

where we take $\gamma = 2$ and $E_0 = 10\,\mathrm{GeV}$.[7] Increasing E_0 negligibly impacts our main results, due to the weak dependence of the CRIR on super-GeV CRs. Further, changing γ between 2 and 3/2 produces no qualitative changes in the results, nor quantitative variations over an order of magnitude. The normalization factor, Q_0, is calculated by assuming

$$\varepsilon_{\rm CR} = \int dV \int_{E_{\rm min}}^{E_{\rm max}} Q(E) dE \tag{9}$$

where $E_{\rm min} = 13.6$ eV and $E_{\rm max} = 100$ GeV. These bounds have a minor impact on the overall results of the work. Determining the injection and maximum energies requires particle-in-cell calculations of the CR acceleration and injection within molecular cloud reconnection zones. However, even if energy losses are ignored, the necessary acceleration timescale from $E_{\rm max} = eBv_{\rm A}^2\delta t$ to accelerate protons up to 100 GeV exceeds molecular cloud lifetimes for much of the parameter space.

The CR proton spectrum from the reconnection zones is a balance of injection and energy losses. The steady-state energy-loss solution (Longair 2011) for the number density of protons within the reconnection region, $\mathcal{N}_p(E)$, is

$$\mathcal{N}_p(E) = \left|\frac{dE}{dt}\right|^{-1} \int_E^{E_{\rm max}} Q(E) dE \tag{10}$$

where $\frac{dE}{dt}$ is calculated using a prescribed loss function, $\mathcal{L}(E)$

$$\frac{dE}{dt} = \mathcal{M}_s^2 n v_{\rm CR}(E) \mathcal{L}(E) \tag{11}$$

and $\mathcal{M}_s$ is the sonic Mach number, $\mathcal{M}_s = \sigma(l)/c_s$, $c_s = \sqrt{k_b T/\mu m_H}$, μ is the mean molecular weight, $T = 10$ K, and $v_{\rm CR}(E)$ is the relativistic velocity of the CR. We utilize the loss function given in Padovani et al. (2009).

Turbulent reconnection is an essential part of the turbulent cascade (Lazarian & Vishniac 1999) and a volume-filling process. This induces CR acceleration and we model the resulting CR number density accelerated by turbulent reconnection at length scale ℓ by assuming the CRs diffuse from the reconnection zones and undergo energy losses. We assume an

[7] This limit was determined by examining the energy-loss and acceleration timescales.

energy-dependent empirical diffusion coefficient[8] (Longair 2011):

$$D(E) = D_0\left(\frac{E}{10\ \mathrm{GeV}}\right)^{\delta}\ \mathrm{cm^2\ s^{-1}} \quad (12)$$

using $\delta = 0.5$ and different values of D_0. The diffusion length scale is defined by

$$\ell_D = D(E)/v_{\mathrm{CR}}(E). \quad (13)$$

The energy-loss scale, or the range, $R(E)$, is given by the stopping column, (Padovani et al. 2009)

$$n \times R(E) = \int_0^E \frac{dE}{\mathcal{L}(E)}\ \mathrm{cm^{-2}}. \quad (14)$$

We then define a transport length scale, ℓ_T,

$$\ell_T^{-1} = \ell_D^{-1} + R^{-1}. \quad (15)$$

Finally, we use the volume-filling fraction of the reconnection zones

$$f_V = V_{\mathrm{rec}}/V_\ell \quad (16)$$

where V_{rec} is the volume of a sheet-like reconnection zone,

$$V_{\mathrm{rec}} = l_{\mathrm{A}}^2\Delta, \quad (17)$$

$l_{\mathrm{A}} = \ell M_{\mathrm{A}}^{-3}$ for super- and trans-Alfvénic turbulence and $l_{\mathrm{A}} = \ell M_{\mathrm{A}}^2$ for sub-Alfvénic turbulence (Lazarian et al. 2020). Following Lazarian & Vishniac (1999) the reconnection zone width is

$$\Delta = l_{\mathrm{A}}\left(\frac{l_{\mathrm{A}}}{\ell}\right)^{0.5}\mathcal{M}_{\mathrm{A}}^2. \quad (18)$$

The volume of a region of radius ℓ is $V_l = \frac{4}{3}\pi\ell^3$. The number density of transported CRs is

$$\mathcal{N}_T(E) = \mathcal{N}_p e^{-\frac{\ell}{\ell_T}}. \quad (19)$$

Either number density, $\mathcal{N}_p(E)$ or $\mathcal{N}_T(E)$, can be converted to a flux by

$$j_{\{p,T\}}(E) = \frac{v_{\mathrm{CR}}(E)\mathcal{N}_{\{p,T\}}(E)}{4\pi}. \quad (20)$$

The resulting CRIR due to turbulent reconnection at length scale, ℓ, is

$$\zeta(\ell) = 4\pi f_V \int_{E_{\mathrm{min}}}^{E_{\mathrm{max}}} j(E)\sigma(E)dE \quad (21)$$

where $\sigma(E)$ is the total ionization cross section. We use the empirical fit from Rudd et al. (1985).

3. Results and Discussion

For the following results, our canonical cloud is virialized, $\alpha_V = 1$, and turbulence is injected at a scale of 1 pc with a turbulent line width of $1\ \mathrm{km\ s^{-1}}$. This results in the cloud primarily being sub-Alfvénic (see, e.g., Crutcher & Kemball 2019). Figure 2 shows the steady-state flux, $j_p(E)$, and the transported flux, $j_T(E)$, as a function of scale ℓ and CR energy, E. Both $Q(E)$ and $j_p(E)$ are weakly dependent on the length scale, ℓ. The CRIR associated with $j_p(E)$ are of order $\zeta \approx 7\times10^{-10}$–$10^{-9}\ \mathrm{s^{-1}}$ (not shown in the figure). These CRIRs are too high to be physical, and highlight the necessity of treating the diffusion of the CRs throughout the rest of the cloud structures.

The final CR spectrum, $j_T(E)$, shows significant variation with both D_0 and ℓ. The flux at low energies is dramatically decreased due to energy losses from ionizations, Coulomb interactions, and pion production, while at high energies the flux is suppressed by diffusion. Our model predicts reconnection will seed the cloud with protons of energies $E \approx 10^6$–10^{10} eV. The resulting spectrum is greatly sensitive to the diffusion coefficient, D_0. For diffusion coefficients $D_0 = 10^{29}$ and $3\times10^{28}\ \mathrm{cm^2\ s^{-1}}$, the resulting spectrum is relatively flat. However, for lower values of D_0, the spectrum is only flat for reconnection driven by the smallest scales of turbulence. We find a significant change in behavior between high D_0 and low D_0 values. For $D_0 = 3\times10^{28}$ and $10^{29}\ \mathrm{cm^2\ s^{-1}}$, we find the flux typically increases with the turbulence driving the length scale, ℓ. For $D_0 = 10^{28}$ and $3\times10^{27}\ \mathrm{cm^2\ s^{-1}}$ the flux decreases with increasing length scales. Conversely, if the particles travel ballistically, the transport length $\ell_T \approx R$ and the CRIR increases dramatically to $\zeta \approx 10^{-14}\ \mathrm{s^{-1}}$ for the fiducial model. This CRIR is far outside the observed range within the Milky Way, except in sightlines toward the Galactic Center (Indriolo et al. 2015). Therefore, in the framework of CR acceleration by magnetic reconnection, low-energy CRs must travel diffusely or the acceleration efficiency must be $f_{\mathrm{CR}} \ll 0.01$ to be consistent with observations.

Figure 3 shows the resulting CRIR, $\zeta(\ell)$ as a function of length scale, ℓ, for different values of D_0. We highlight in the blue box the range of inferred values of ζ for molecular clouds in the Milky Way. We find that for values of $D_0 > 10^{28}\ \mathrm{cm^2\ s^{-1}}$, our model is able to produce (or overproduce) the CRIR inferred in molecular clouds. For low values of D_0, the CRIR is below even the effective minimum ionization rate $\approx 10^{-19}$ in molecular clouds due to radioactive nuclei decay (Adams et al. 2014).

Table 1 shows the power-spectrum-averaged CRIR, defined as

$$\zeta_W = \frac{\int_{2\pi/L}^{k_{\mathrm{max}}} W(k)\zeta(\ell)k^2dk}{\int_{2\pi/L}^{k_{\mathrm{max}}} W(k)k^2dk} \quad (22)$$

where $k = 2\pi/\ell$ and $W(k)$ is the isotropic kinetic energy turbulence spectrum

$$W(k) = \frac{\rho\sigma(k)^2}{2k} \quad (23)$$

and $\sigma(k) = \sigma_0\left(\frac{k_0}{k}\right)^{\beta}$. We find that for all cases, increasing D_0 (and thus allowing CRs to propagate more easily throughout the cloud) systematically increases the CRIR. For the "less bound" clouds, the ionization rate increases due to the decreased average density, and hence CRs lose less energy through the cloud. Similarly, for both the "strong turbulence"

[8] The process of CR diffusion in MHD turbulence is pretty complicated with different components of MHD modes acting very differently on CRs (see Yan & Lazarian 2004) and its effects for the diffusion parallel and perpendicular to the mean magnetic field is also not trivial (see Lazarian & Yan 2014). However, for the sake of simplicity, in this paper we adopt the simplest possible assumptions about the diffusion. This assumption is further justified by Lazarian & Xu (2021), who presented a new nonresonant scattering process in turbulent magnetized media.

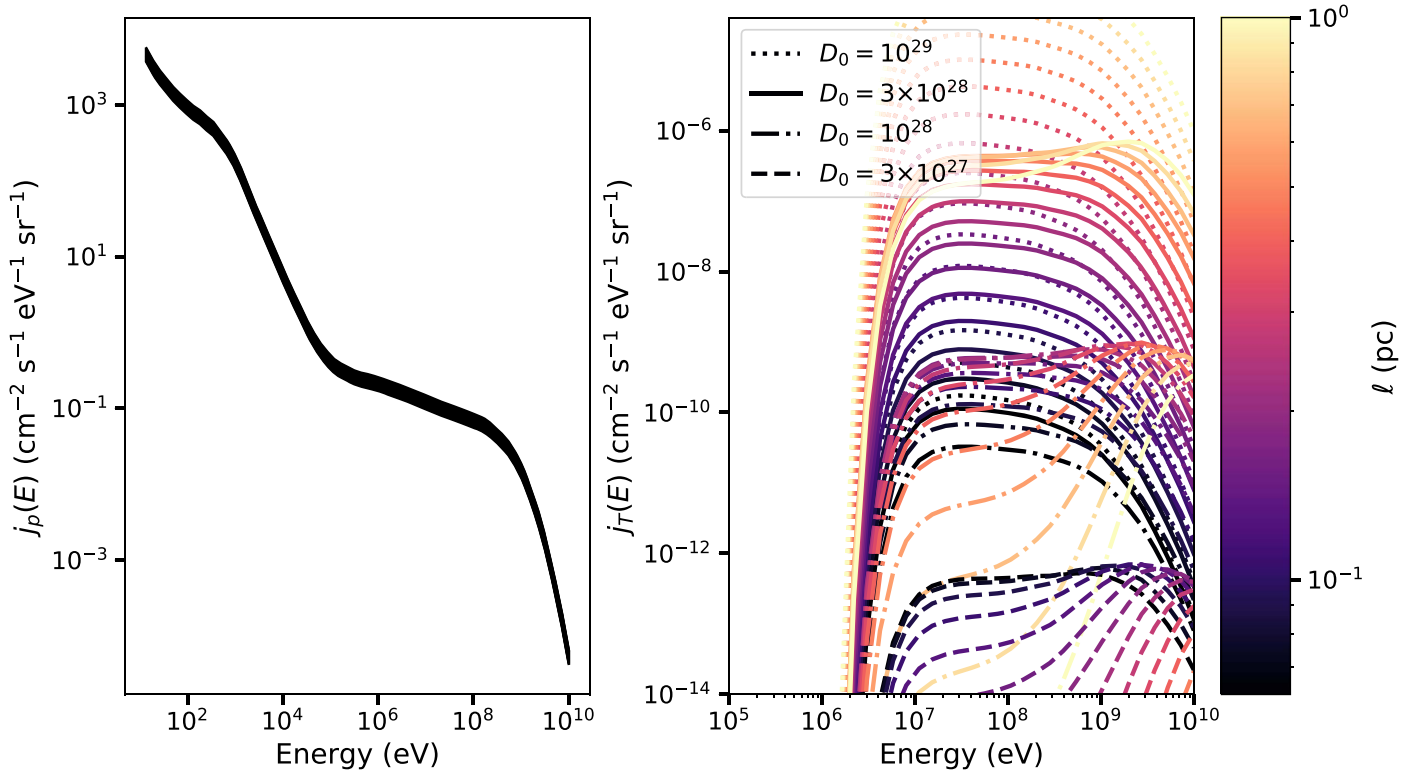

Figure 2. Left: steady-state solution for the flux, $j_p(E)$ as a function of energy for different values of ℓ. Right: transported cosmic-ray flux, $j_T(E)$, as a function of energy for different values of D_0 and ℓ. Note the different scales for the x- and y-axes of each panel. Without including the impact of energy losses and diffusion throughout the cloud, the resulting cosmic-ray flux would produce nonphysically high ionization rates.

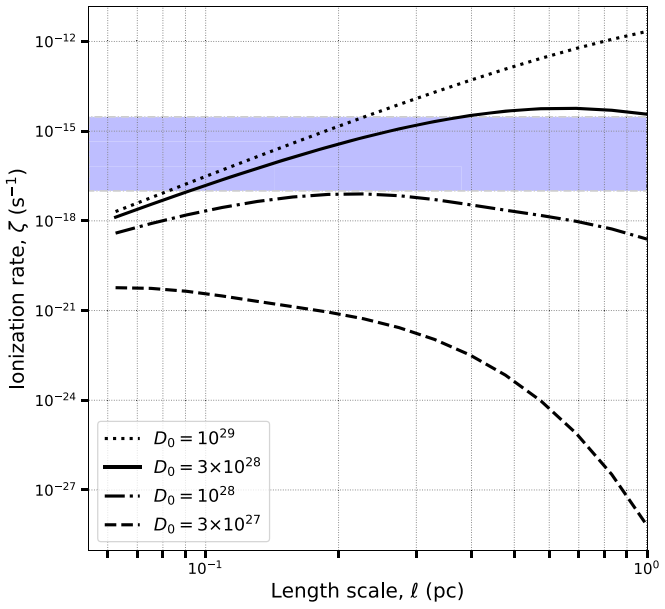

Figure 3. Cosmic-ray ionization rate, $\zeta(\ell)$, due to turbulent reconnection from turbulence at length scale, ℓ, accounting for diffusion and energy losses.

model and "Kolmogorov turbulence" model, for which the turbulence strength is not increased, the produced CRIR is increased due to the enhanced turbulent power throughout the driving scales.

Our "strong turbulence" model represents regions of significant driving, such as in regions of enhanced star formation feedback (e.g., Offner & Liu 2018) (e.g., nearby protostar jets, high-mass stars, and supernovae) or in the Galactic Center (Kauffmann et al. 2017). Due to the strength of the turbulence, there is a significantly enhanced CRIR produced, far exceeding that observed in solar neighborhood clouds. However, CRIRs on the order of 10^{-14} s^{-1} are observed through H_3^+ absorption toward the Galactic Center (Indriolo et al. 2015).

Most of the clouds in the Milky Way are not entirely virialized, and exhibit virial parameters greater than 1 (Heyer & Dame 2015). Therefore, our model predicts that within these clouds, reconnection within the MHD turbulence produces enough MeV–GeV protons to sustain CRIRs, $\zeta > 10^{-16}$ s^{-1}.

This mechanism directly correlates the CRIR and the properties of the MHD turbulence within molecular clouds, along with the transport physics of low-energy CRs. Therefore, it may be possible to verify this mechanism with cospatial

Table 1
Power-spectrum-averaged Cloud Ionization Rates

$D_0 =$	3×10^{27}	1×10^{28}	3×10^{28}	1×10^{29}
Fiducial	↓	9.1(−19)	7.5(−17)	2.5(−15)
Less Bound	↓	2.8(−18)	2.3(−16)	8.0(−15)
Strong Turb.	2.9(−18)	1.1(−15)	6.2(−14)	6.7(−13)
Kolmogorov Turb.	↓	1.1(−17)	1.7(−16)	1.6(−15)

Note. The power-spectrum-averaged cloud cosmic-ray ionization rates (s^{-1}), ζ_W, (Equation (22)) for different values of D_0. The value in the parenthesis indicates the power. The fiducial model uses the parameters $\alpha_V = 1$, $\beta = 0.5$, $\sigma_0 = 1$ km s^{-1}, and $L = 1$ pc. The rest of the rows delineate models with a specific parameter variation: "Less Bound" corresponds to $\alpha_V = 2$, "Strong Turbulence" to $\sigma_V = 2.5$ km s^{-1}, and "Kolmogorov Turbulence" to $\beta = 0.33$. The ↓ represents ionization rates below the radionuclide ionization rate (Adams et al. 2014), $\zeta_{RN} \approx 10^{-19}$.

observations of the ionization rate in dense gas, the magnetic field strength, and the turbulence properties through observations of molecular ions and dust polarization maps. However, inferring the CRIR from such observations will rely on understanding the diffusion coefficient. Conversely, if the CRIR is dominated in dense gas by our proposed mechanism, it may be possible to infer the properties of the MHD turbulence from the CRIR through backwards modeling.

It is worth discussing the great uncertainty in the diffusion coefficient. Within the Milky Way, CR transport studies and observations have indicated an average diffusion coefficient between $D_0 = 10^{28}$–$3 \times 10^{28}\,\mathrm{cm^2\,s^{-1}}$ (Evoli et al. 2020). However, regarding the dense gas, studies have shown a spread over several orders of magnitude, from $D_0 = 10^{27}$–$10^{30}\,\mathrm{cm^2\,s^{-1}}$ (Dogiel et al. 2015; Owen et al. 2021). As such, it is even more paramount to understand what is constraining the CR transport within molecular gas, and how the local environment changes the diffusion coefficient. Therefore, a wide spread is observed, although dwarf galaxies appear to necessitate a higher ionization rate. If this is the case, our model predicts that dwarf galaxies would have CRIRs significantly greater than Milky Way–type galaxies.

We have proposed a novel mechanism for the production of low-energy CRs in molecular clouds through Fermi acceleration in regions undergoing turbulence reconnection: Cosmic-Ray Acceleration From Turbulence (CRAFT). Since the MHD turbulence cascades across a wide range of scales, and since both the turbulence and the reconnection are volume-filling processes, we expect this will produce an approximately isotropic and homogenous floor to the CRIR. Historically, there has been a contradiction between the constant CRIRs used in astrochemical models (Röllig et al. 2007) and theoretical calculations that have ubiquitously shown that energy losses would produce steep gradients with a low CRIR toward the clouds center. Furthermore, observations indicate the ionization rate in dense gas is not significantly lower than in more diffuse regions. Our results would instead show that a properly chosen constant CRIR may be actually appropriate when modeling the dense gas in molecular clouds.

We thank the anonymous referee for their useful comments improving this work. This work was funded by the ERC starting grant No. 679852 “RADFEEDBACK.” A.L. acknowledges the support by NASA TCAN AAG1967 and NSF AST 1816234. B.A.L.G would also like to thank his canine office mate, Mojo Gaches, for providing constant support during this work during the Coronavirus pandemic, although due to constantly sleeping on the job is not a co-author.

ORCID iDs

Brandt A. L. Gaches https://orcid.org/0000-0003-4224-6829
Stefanie Walch https://orcid.org/0000-0001-6941-7638
A. Lazarian https://orcid.org/0000-0002-7336-6674

References

Adams, F. C., Fatuzzo, M., & Holden, L. 2014, ApJ, 789, 86
Barger, C. J., & Garrod, R. T. 2020, ApJ, 888, 38
Caselli, P., Walmsley, C. M., Terzieva, R., & Herbst, E. 1998, ApJ, 499, 234
Ceccarelli, C., Dominik, C., López-Sepulcre, A., et al. 2014, ApJL, 790, L1
Crutcher, R. M., & Kemball, A. J. 2019, FrASS, 6, 66
Dalgarno, A. 2006, PNAS, 103, 12269
de Gouveia dal Pino, E. M., & Lazarian, A. 2005, A&A, 441, 845
Dogiel, V. A., Chernyshov, D. O., Kiselev, A. M., et al. 2015, ApJ, 809, 48
Evoli, C., Morlino, G., Blasi, P., & Aloisio, R. 2020, PhRvD, 101, 023013
Eyink, G., Vishniac, E., Lalescu, C., et al. 2013, Natur, 497, 466
Eyink, G. L., Lazarian, A., & Vishniac, E. T. 2011, ApJ, 743, 51
Favre, C., Ceccarelli, C., López-Sepulcre, A., et al. 2018, ApJ, 859, 136
Favre, C., López-Sepulcre, A., Ceccarelli, C., et al. 2017, A&A, 608, A82
Fujita, Y., Nobukawa, K. K., & Sano, H. 2021, ApJ, 908, 136
Gaches, B. A. L., & Offner, S. S. R. 2018, ApJ, 861, 87
Heyer, M., & Dame, T. M. 2015, ARA&A, 53, 583
Indriolo, N., & McCall, B. J. 2012, ApJ, 745, 91
Indriolo, N., Neufeld, D. A., Gerin, M., et al. 2015, ApJ, 800, 40
Ivlev, A. V., Dogiel, V. A., Chernyshov, D. O., et al. 2018, ApJ, 855, 23
Kauffmann, J., Pillai, T., Zhang, Q., et al. 2017, A&A, 603, A89
Khiali, B., de Gouveia Dal Pino, E. M., & del Valle, M. V. 2015, MNRAS, 449, 34
Kowal, G., de Gouveia Dal Pino, E. M., & Lazarian, A. 2011, ApJ, 735, 102
Larson, R. B. 1981, MNRAS, 194, 809
Lazarian, A., Eyink, G. L., Jafari, A., et al. 2020, PhPl, 27, 012305
Lazarian, A., & Vishniac, E. T. 1999, ApJ, 517, 700
Lazarian, A., & Xu, S. 2021, arXiv:2106.08362
Lazarian, A., & Yan, H. 2014, ApJ, 784, 38
Longair, M. S. 2011, High Energy Astrophysics (Cambridge: Cambridge Univ. Press)
McKee, C. F., & Ostriker, E. C. 2007, ARA&A, 45, 565
Meng, F., Sánchez-Monge, Á, Schilke, P., et al. 2019, A&A, 630, A73
Morlino, G., & Gabici, S. 2015, MNRAS, 451, L100
Neufeld, D. A., & Wolfire, M. G. 2017, ApJ, 845, 163
Offner, S. S. R., & Liu, Y. 2018, NatAs, 2, 896
Owen, E. R., On, A. Y. L., Lai, S.-P., & Wu, K. 2021, ApJ, 913, 52
Padovani, M., Galli, D., & Glassgold, A. E. 2009, A&A, 501, 619
Padovani, M., Ivlev, A. V., Galli, D., et al. 2020, SSRv, 216, 29
Padovani, M., Marcowith, A., Hennebelle, P., & Ferrière, K. 2016, A&A, 590, A8
Padovani, M., Marcowith, A., Sánchez-Monge, Á., Meng, F., & Schilke, P. 2019, A&A, 630, A72
Phan, V. H. M., Morlino, G., & Gabici, S. 2018, MNRAS, 480, 5167
Röllig, M., Abel, N. P., Bell, T., et al. 2007, A&A, 467, 187
Rudd, M. E., Kim, Y. K., Madison, D. H., & Gallagher, J. W. 1985, RvMP, 57, 965
Schlickeiser, R. 2002, Cosmic Ray Astrophysics (Berlin: Springer)
Schlickeiser, R., Caglar, M., & Lazarian, A. 2016, ApJ, 824, 89
Silsbee, K., & Ivlev, A. V. 2019, ApJ, 879, 14
Yan, H., & Lazarian, A. 2004, ApJ, 614, 757
Yang, R.-Z., & Wang, Y. 2020, A&A, 640, A60